J. Membrane Biol. 114, 231–243 (1990)

The Journal of
Membrane Biology

Macroscopic and Single-Channel Studies of Two Ca^{2+} Channel Types in Oocytes of the Ascidian *Ciona intestinalis*

Martha M. Bosma† and William J. Moody‡
†Department of Physiology and Biophysics, and ‡Department of Zoology, University of Washington, Seattle, Washington, 98195

Summary. Whole-cell and single-channel patch-clamp experiments were performed on unfertilized oocytes of the ascidian *Ciona intestinalis* to investigate the properties of two voltage-dependent Ca^{2+} currents found in this cell. The peak of the low threshold current (channel I) occurred at −20 mV, the peak of the high-threshold current (channel II) at +20 mV. The two currents could be distinguished by voltage dependence, kinetics of inactivation and ion selectivity. During large depolarizing voltage pulses, a transient outward current was recorded which appeared to be due to potassium efflux through channel II. When the external concentrations of Ca^{2+} and Mg^{2+} were reduced sufficiently, large inward Na currents flowed through both channels I and II. Using divalent-free solutions in cell-attached patch recordings, single-channel currents representing Na influx through channels I and II were recorded. The two types of unitary events could be distinguished on the basis of open time (channel I longer) and conductance (channel I smaller). Blocking events during channel I openings were recorded when micromolar concentrations of Ca^{2+} or Mg^{2+} were added to the patch pipette solutions. Slopes of the blocking rate constant *vs.* concentration gave binding constants of 6.4×10^6 M^{-1} sec^{-1} for Mg^{2+} and 4.5×10^8 M^{-1} sec^{-1} for Ca^{2+}. The Ca^{2+} block was somewhat relieved at negative potentials, whereas the Mg^{2+} block was not, suggesting that Ca^{2+}, but not Mg^{2+}, can exit from the binding site toward the cell interior.

Key Words oocyte · calcium channel · single channel · development · tunicate

Introduction

Although Ca^{2+} currents in oocytes have been studied extensively (*see* e.g., Hagiwara, Ozawa & Sand, 1975; Yoshida, 1983; Hirano & Takahashi, 1984), no analysis has been done at the single-channel level. Since the properties and distribution of Ca^{2+} channels in embryos are known to change during early development (Hirano & Takahashi, 1984; Simoncini, Block & Moody, 1988), such analysis is important because it permits comparison of the biophysical properties of Ca^{2+} channels expressed at the earliest stages of development with those in terminally differentiated cells. This is a first step in analyzing how the process of development acts on ion channel properties to create the electrophysiological diversity of mature cell types.

The existence of multiple types of calcium channels in individual cells was first demonstrated in starfish oocytes (Hagiwara et al., 1975) and has since been described in a wide variety of preparations (Deitmer, 1984; Fedulova, Kostyuk & Veselovsky, 1985; Matteson & Armstrong, 1986; Fox, Nowycky & Tsien, 1987; Narahashi, Tsunoo & Yoshii, 1987; *see* Tsien et al., 1988, for review). The Ca^{2+} channel types are generally distinguishable by the voltage dependence and kinetics of the macroscopic currents, by conductance and kinetics of the single-channel events, by permeability sequence, and by differential sensitivity to toxins and to dihydropyridine drugs. Recent work has explored the permeation mechanisms of Ca^{2+} channels in detail, and has shown that in the absence of divalent cations in the external solution, monovalent cations can pass through Ca^{2+} channels (Kostyuk & Krishtal, 1977; Yoshida, 1983; Almers, McCleskey & Palade, 1984; Hess & Tsien, 1984; Fukushima & Hagiwara, 1985; Hess, Lansman & Tsien, 1986). The inverse relation between the permeabilities of various ions in the Ca^{2+} channel, as judged by reversal potentials, and their mobilities, as judged by single-channel conductance, indicates that permeation must involve a binding step (Hess & Tsien, 1984; Fukushima & Hagiwara, 1985). Because the Ca^{2+} concentration required to block monovalent permeation through the channel is several orders of magnitude less than that required to saturate channel conductance, permeation models are based on at least two binding sites within the channel (Kostyuk, Mironov & Shuba, 1983; Almers & McCleskey, 1984; Hess & Tsien, 1984; Fukushima & Hagiwara, 1985; Lansman, Hess & Tsien, 1986).

The permeation of monovalent ions through

multiple Ca^{2+} channel types has seldom been studied in individual cells. It has also been difficult in most preparations to record whole-cell currents and control absolute membrane potential at the same time as measuring single-channel currents with cell-attached patch pipettes (*see* Lux & Brown, 1984; Hirano & Hagiwara, 1989). In the experiments reported here, we have used oocytes of the ascidian *Ciona intestinalis*, which have two voltage-dependent Ca^{2+} currents (Hice, 1988), to do both. We have identified unitary events corresponding to two Ca^{2+} currents in *Ciona* oocytes, shown that monovalent ions permeate through both when external divalent levels are reduced sufficiently, and determined binding constants at the single-channel level for the block of monovalent permeation through one of the channel types by Ca^{2+} and Mg^{2+} ions.

Materials and Methods

All experiments were carried out in the Department of Physiology at the University of Bristol, Bristol, England. *Ciona intestinalis* were collected at the Marine Biological Laboratory, Plymouth, England, and were maintained at Bristol at 12°C in a mixture of natural and artificial seawater. Post-vitellogenic oocytes were removed surgically from the oviduct. The chorion was removed manually using electrolytically sharpened tungsten needles. Experiments were carried out at 10–12°C; oocytes were continuously superfused with solution during the experiments.

Solutions

Artificial seawater (ASW) contained (in mM): NaCl, 500; KCl, 10; $CaCl_2$, 10; $MgCl_2$, 69; buffered to pH 8.0 with 10 mM HEPES (N-(2-hydroxyethyl)piperazine-N′-(2-ethanesulfonic acid)) with added NaOH. ASW with increased permeant divalent levels contained 50 mM of either $CaCl_2$ or $BaCl_2$, plus 29 mM $MgCl_2$. Internal solution for whole-cell recording contained (in mM): KCl, 400; $MgCl_2$, 5; NaCl, 10; BAPTA (1,2-*bis*(2-aminophenoxy)-ethane-N,N,N′,N′-tetraacetic acid), 2; buffered to pH 7.3 with 20 mM HEPES plus added KOH. Since whole-cell recordings were carried out with pipettes that were small in relation to the cell diameter (*see below*), exchange of solution and rundown of currents were minimal during an experiment. The base solution for studying the effects of reduced external divalents in patch and whole-cell experiments contained 618 mM NaCl, 0 mM $CaCl_2$, 0 mM $MgCl_2$, with 2 mM BAPTA or EGTA (ethyleneglycol-*bis*(B-aminoethyl ether) N,N,N′,N′-tetraacetic acid). To this was added $MgCl_2$ at concentrations between 50 μM and 2 mM, or $CaCl_2$ in amounts calculated to give free calcium concentrations between 0.1 and 1.0 μM, using a dissociation constant for BAPTA of 0.107 μM (Tsien, 1980). All solutions were filtered at 0.22 μm immediately before use.

Electrophysiological Methods

Pipettes for whole-cell clamp were pulled from borosilicate hematocrit glass tubing to diameters of 2–5 μm using a two-stage pull. Whole-cell clamp methods (Hamill et al., 1981) give adequate voltage clamp of ascidian oocytes, even using pipettes which are small in relation to the cell diameter (160 μm), because like many oocytes, these cells have a very high membrane resistance and a low density of voltage-dependent currents (*see* Block & Moody, 1987, for a more detailed discussion). Pipettes for single-channel recording were slightly smaller, except for cases in which we wished to record from patches containing fairly large numbers of channels (*see* Fig. 8). Pipettes used for single-channel recording were coated with polystyrene dissolved in toluene to reduce capacitance. All pipettes were fire polished immediately before use.

In all single-channel experiments, whole-cell clamp and attached-patch recordings were carried out simultaneously using List EPC-5 and EPC-7 amplifiers. In this way, absolute potentials were known with greater certainty and voltage pulses could be delivered through the whole-cell pipette, minimizing charging and leakage artifacts across the patch pipette wall and seal resistance. In addition, by using this method, whole-cell and single-channel currents could be recorded simultaneously. Single-channel data were filtered at 2.9 kHz with an 8-pole Bessel characteristic, and were stored both on FM magnetic tape and and in digital form on a laboratory microcomputer. Whole-cell current and voltage data were stored on FM magnetic tape for later analysis. Analysis was carried out using one of three software packages (CED, Cambridge, England; PCLAMP, Axon Instruments, Burlingame, CA; or custom written software). Records for single-channel analysis were digitized at 10 kHz (12-bit resolution); single-channel events were detected using a half-maximum amplitude criterion.

Results

Properties of Two Calcium Currents in the Unfertilized Oocyte

Whole-cell voltage-clamp records from unfertilized oocytes of *Ciona intestinalis* revealed two inward calcium currents. These are illustrated in Fig. 1*A* (top set of traces), which show currents recorded during depolarizing voltage-clamp steps taken from a holding potential of −80 mV. A low threshold current (channel I) appeared at voltages of −40 to 0 mV, with peak current recorded at −30 to −10 mV. The channel I current showed relatively slow activation and inactivation; inactivation kinetics were well described by a single exponential time course, with a time constant in the range of 400–500 msec at −20 mV. At potentials more positive than 0 mV, a second calcium current was seen (channel II). The peak channel II current was recorded at +20 to +30 mV. It showed more rapid inactivation kinetics, which were best described by the sum of two exponentials, with time constants of 32–50 and 450–750 msec at +20 mV. The slow component of channel II inactivation could not be readily explained by residual channel I current, since (*i*) the kinetics were slower and the amplitude larger than would be pre-

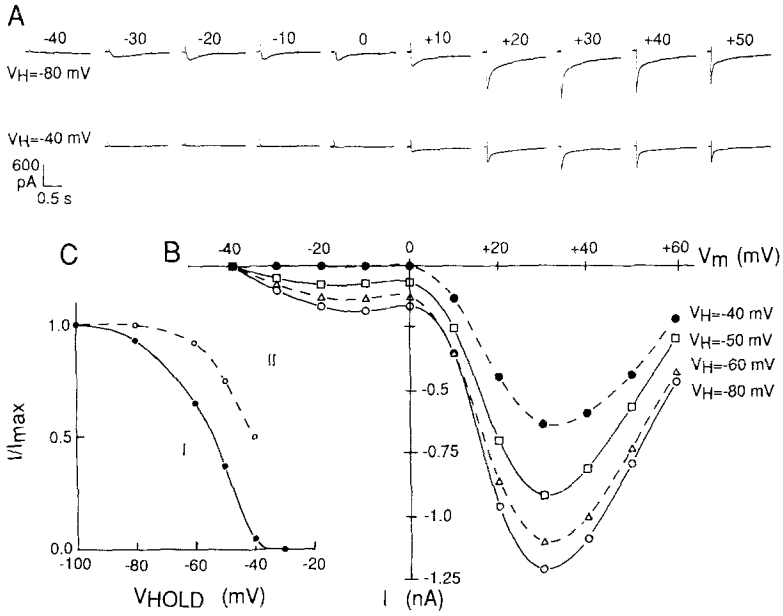

Fig. 1. Two Ca^{2+} currents in the unfertilized *Ciona* oocyte. (*A*) Current records recorded during voltage-clamp pulses to the potentials indicated from a holding potential of either −80 mV (top row of traces) or −40 mV. Each sweep is 1600 msec in duration. (*B*) Current-voltage relations for the peak inward current from the same oocyte taken from holding potentials of −40, −50, −60 and −80 mV. (*C*) Steady-state inactivation *vs.* voltage curves for channel I and II currents from the same cell. Peak currents during test pulses to −10 and +30 mV were measured after a 10-sec prepulse to the voltages indicated. All experiments were done in 50 mM Ca^{2+}

dicted from the properties of channel I currents at more negative potentials, and (*ii*) it was observed in cells which had no detectable channel I current. The channel I current appeared in the *I-V* relation as a shoulder at low voltages, or more often as a distinct peak, so that the *I-V* relation showed a local minimum at 0 to −10 mV.

Channel I and II currents could be separated readily because of differences in the voltage dependence of steady-state inactivation. Figure 1*A* compares currents recorded during depolarizing voltage-clamp steps from holding potentials of −80 and −40 mV. The results of this experiment are plotted as current-voltage and steady-state inactivation *vs.* voltage relations in Fig. 1*B* and *C*. The channel I current was completely inactivated at holding potentials of −40 to −50 mV (50 mM Ca^{2+}). These holding potentials reduced the channel II current by less than 50%. Similar results were obtained in three other cells in which complete h_∞ curves were obtained, and 11 others in which *I-V* relations from two holding potentials were determined.

In our sample of 27 oocytes, channel II current was in all but one case (*see* Fig. 8*B*) larger than channel I current. Channel I current ranged in peak amplitude from 0–1200 pA with a mean of about 200 pA (50 Ca ASW); channel II current ranged from 50–1800 pA, with a mean of about 700 pA. There was no correlation between the amplitudes of the two currents.

In addition to differences in voltage dependence of activation and inactivation, and kinetics, channel I and II currents could be distinguished by their different selectivity for divalent cations. Figure 2 shows voltage-clamp records and *I-V* relations obtained in 50 Ca and 50 Ba external solutions. In 50 Ba, the channel I current was increased by a factor of 7.4, while the channel II current was increased by only 1.14. In two other cells, substitution of 50 Ba for 50 Ca increased channel I current by 4.0 and 2.5-fold, and channel II current by 1.03 and 1.2. The source of this variability is not clear.

There was little change in the kinetics of either current when Ba^{2+} was substituted for Ca^{2+}. Both currents showed inactivation, and in some cells the rates of inactivation were slightly increased in Ba^{2+}. This suggests that inactivation of both currents is voltage- rather than calcium-dependent. This is confirmed by the persistence of inactivation when monovalent cations carry the inward currents through both channels (*see below*).

Monovalent Efflux Through Channel II at Positive Potentials

In many cell types, including oocytes, efflux of monovalent cations through Ca^{2+} channels occurs at positive voltages, and represents a substantial fraction of the total outward current recorded at these potentials (Lee & Tsien, 1982; Fukushima & Hagiwara, 1985; Peres, 1987). Monovalent efflux is thought to occur because of the voltage-dependent removal of divalent cations from a binding site within the channel which, when occupied, normally prevents permeation of monovalent ions (*see* Fukushima & Hagiwara, 1985). In *Ciona* oocytes, a transient outward current was seen at voltages posi-

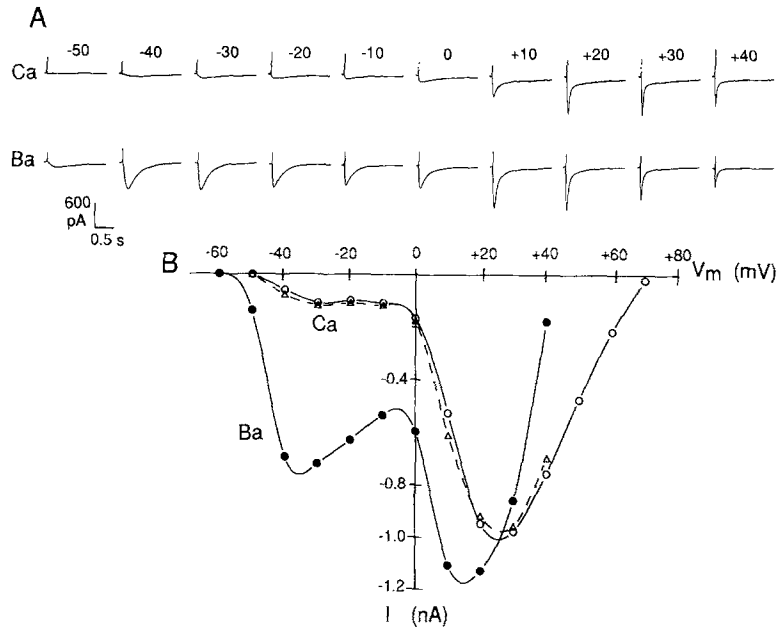

Fig. 2. Differential effects of Ba^{2+} substitution for Ca^{2+} in the external solution on channel I and II currents. (*A*) Current records recorded during voltage-clamp pulses to the potentials indicated from a holding potential of −80 mV with either 50 mM Ca^{2+} (top row) or Ba^{2+} (bottom row) in the external solution. Individual traces are 1600 msec in duration. (*B*) Current-voltage relations from the same cell in 50 mM Ca^{2+} (○), 50 mM Ba^{2+} (●) and return to Ca^{2+} (△)

tive to +50–+80 mV, with either Ba^{2+} or Ca^{2+} as the charge carrier (Fig. 3). A number of properties of this outward current indicate that it represents monovalent efflux, primarily through channel II.

(*i*) At the reversal potential, the current record was invariably flat, showing no time-dependent components (Fig. 3*A*). This would not be expected if the outward current flowed through voltage-dependent channels separate from those carrying the inward current, since it is unlikely that the kinetics of the two channel populations would be identical at the voltage where the currents were equal and opposite. Time invariant current was recorded at the reversal potential between inward and outward currents in 50 Ba, 50 Ca or divalent-free external solutions, even though the absolute potential at which reversal occurred varied by almost 40 mV in these three solutions (*see below*).

(*ii*) The steady-state inactivation *vs.* voltage relations for the outward current and the channel II inward current were identical. Figure 3*B* and *C* show *I-V* relations taken from various holding potentials, and the resulting h_∞ curves for inward and outward currents from a cell which showed very little channel I inward current. Best fits to the two h_∞ curves gave $V_{1/2}$ values of −45 mV for the channel II inward current (filled symbols) and −46 mV for the outward current (open symbols). The $V_{1/2}$ value for channel I inward current is more negative than this by 10–27 mV (*see* Fig. 1*C*). Similar results were obtained from cells which showed substantial channel I currents.

(*iii*) The inactivation kinetics of the outward current were very similar to those of the channel II inward current. Figure 3*D* shows half-inactivation times for the channel II inward and outward currents plotted *vs.* voltage, with the reversal potential indicated by the arrow. The extrapolation of the line drawn through the inward current points predicts the half-inactivation times for the outward currents well.

These data argue first, that the transient outward current is not carried through a separate channel, and second, that the majority of the outward current is carried through channel II. This does not imply that outward current cannot flow through channel I; the fact that the outward current is carried primarily through channel II may simply reflect the greater number of these channels in the membrane.

When Ba^{2+} replaced Ca^{2+} in the external solution, the reversal potential shifted to more negative potentials (+55 ± 7.0 mV *vs.* +72 ± 3.4 mV) and the outward current was substantially increased. This is consistent with data for Ca^{2+} channels in myeloma cells (Fukushima & Hagiwara, 1985) and cardiac muscle (Hess et al., 1986), and with a model in which the lower relative permeability of Ba^{2+} reflects its lower binding affinity to a site within the channel, and hence its easier removal from that site at positive voltages, leading to larger outward currents.

Permeation of Monovalent Cations Through Channels I and II with Reduced Levels of External Divalent Cations

In 10 experiments we exposed oocytes to external solutions with greatly reduced levels of Ca^{2+} and

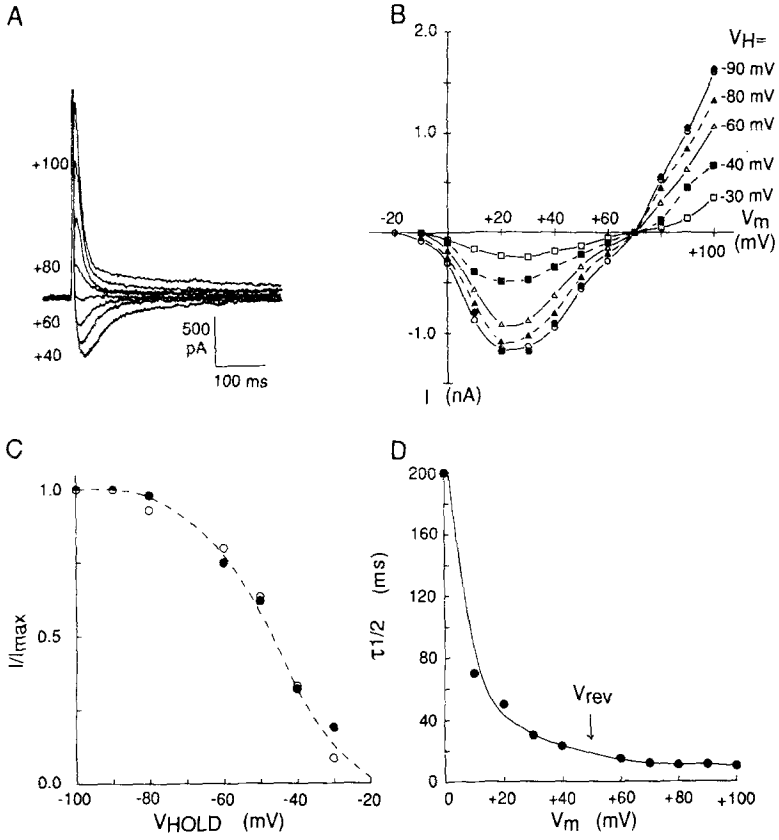

Fig. 3. Monovalent efflux through channel II. (*A*) Inward and outward currents recorded in 50 mM Ba^{2+} during voltage-clamp steps to +20 to +90 (10-mV increments) from a holding potential of −80 mV. (*B*) Current-voltage relations taken in 50 mM Ca^{2+} from holding potentials of −100, −90, −80, −60, −40 and −30 mV. These relations were leak-corrected; estimated leak at the reversal potential (+70 mV) was 125 pA. (*C*) Steady-state inactivation *vs.* voltage curve for inward channel II current (●; +30 mV) and peak outward current (○; +90 mV). Data from cell in *B*. (*D*) Half-inactivation times in 50 mM Ba^{2+} plotted *vs.* voltage from the records in *A*. The arrow indicates the reversal potential, so that channel II inward currents are shown to the left of the arrow and outward currents to the right

Mg^{2+} to see whether under these conditions we could detect Na^+ permeation through either or both calcium channels. These experiments were hampered by the fact that *Ciona* oocytes rarely survived for more than a few minutes in solutions with Ca^{2+} buffered to micromolar levels and Mg^{2+} reduced to less than 2 mM. This made it impossible to determine titration curves from macroscopic currents for the block of Na permeation by Ca^{2+} or Mg^{2+} in single cells (Almers et al., 1984). It also probably caused us to underestimate the magnitude of Na^+ currents through the Ca^{2+} channels because we could not expose cells to reduced divalent levels long enough to ensure that the Ca^{2+} concentration at the cell surface was buffered completely to the nominal value in the bulk solution.

Nonetheless, our results clearly showed that when external Ca^{2+} and Mg^{2+} are reduced sufficiently, both channels I and II become permeant to Na^+, and that the Na^+ currents under such conditions are substantially larger than the Ca^{2+} currents recorded in control external solutions. Figure 4 shows voltage-clamp records and *I-V* relations from a cell exposed first to an external solution with elevated Ca^{2+} (50 mM Ca, 29 mM Mg), and then to a reduced divalent solution (0 mM Ca, 1 mM Mg, 1 mM EGTA). In each of the 10 cells, large inward Na currents through both channels I and II were recorded in the reduced divalent solutions. In the cell shown in Fig. 4, the Na^+ currents were larger than the Ca^{2+} currents in 50 mM Ca for both channels, by a factor of about 16 for channel I and 7 for channel II. During the solution changes in several such experiments, we consistently saw the amplitude of both calcium currents decrease, as Ca^{2+} was removed, and then rapidly increase, as Ca^{2+} and Mg^{2+} fell sufficiently to permit Na^+ permeation.

The following properties of Na^+ currents through the Ca^{2+} channels were consistently observed:

(*i*) Na^+ currents through Ca^{2+} channels were larger in this range of divalent concentrations (nominally 0 mM Ca^{2+}, <2 mM Mg^{2+}) than Ca^{2+} currents even in elevated (50 mM) Ca^{2+} solutions. They were larger by factors of 3.2–33.6 (compared to currents in 50 mM external Ca^{2+}) for channel I, and 4.2–8 for channel II (*see* the Table), although the macroscopic conductance for Ca^{2+} may be underestimated in these experiments because of the presence of 29 mM Mg^{2+} in the 50 mM Ca^{2+} solution. Although titration curves could not be done in single cells, the data in the Table are sufficient to indicate that apparent binding constants are in the micromolar range for Ca^{2+} and the low millimolar range for Mg^{2+}. These correspond well with the estimates based on single-channel recording pre-

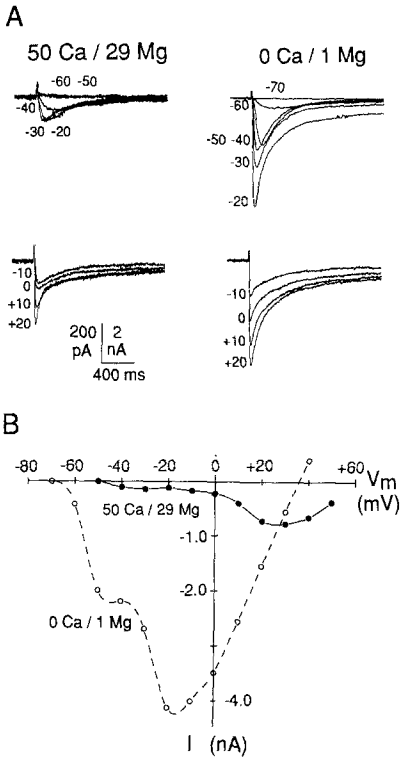

Fig. 4. Monovalent influx through channel I and II in reduced-divalent external solution. (*A*) Current records taken during voltage-clamp pulses to the potentials indicated in high-Ca ASW (50 Ca/29 Mg; left column; $V_{hold} = -80$ mV) and reduced-divalent ASW (0 Ca/1 Mg; right column, $V_{hold} = -100$ mV). Note that the current calibration represents 200 pA for the 50 Ca/29 Mg traces and 2 nA for the 0 Ca/1 Mg traces. (*B*) Current-voltage relations from the same cell in 50 Ca/29 mg and 0 Ca/1 Mg

sented below. The data also suggest some difference between the two channels both in the $Na^+ : Ca^{2+}$ conductance ratio (larger for channel I), and in the titration curve for Mg^{2+} block of Na^+ permeation (channel I more sensitive to Mg^{2+}).

(*ii*) There was a negative shift along the voltage axis in the *I-V* relation in reduced divalent solutions (Fig. 4*B*). This averaged about −30 mV measured at the peak channel II current. This is consistent with a change in surface charge screening resulting from reduction of divalent levels.

(*iii*) The reversal potential between inward and outward currents through channel II shifted in the negative direction from +72 ± 3.3 mV ($n = 9$) in 50 Ca to +36 ± 5.8 mV ($n = 6$) in low divalent solutions. Outward currents were much larger in low divalent solutions. Both effects are consistent with the removal of Ca^{2+} or Mg^{2+} from a binding site in the channel that prevents monovalent flux. At normal external divalent levels, V_{rev} reflects a complex interaction between voltage and divalent concentration in determining the occupancy of this site by Ca^{2+} or Mg^{2+} (*see* Fukushima & Hagiwara, 1985). At low external divalents, V_{rev} more closely reflects

Table. Effect of divalent levels on Na currents through channels I and II

External divalents		Factor increase in macroscopic current	
$[Ca^{2+}]$	$[Mg^{2+}]$	Channel I	Channel II
0	1 mM	30.0, 30.0, 33.6	5.5, 7.2, 5.5
0	2 mM	7.2, 17.0	7.5, 8.0
10^{-7} M	2 mM	6.3, 5.16	
10^{-6} M	2 mM	3.2, 3.4	4.2, 5.0

a permeability ratio for monovalent ions in the channel, in this case Na^+ and K^+. Based on a mean V_{rev} under these conditions of +38 mV, and assuming $[Na^+]_i = 10$ mM and $[K^+]_i = 200$ mM (Hagiwara & Yoshii, 1979), a P_{Na}/P_K ratio for channel II can be calculated to be 2.2. This is very close to the value of 2.57 given by Tsien et al. (1987) for the cardiac Ca^{2+} channel.

(*iv*) Both channel I and II current showed inactivation when Na^+ was the permeant ion. This is consistent with inactivation of currents in Ba^{2+}-containing external solutions and implies that inactivation of both channels is voltage dependent. The kinetics of inactivation were somewhat altered when Na^+ was the permeant ion. The major effect was that the slow component of channel II inactivation contributed relatively more to the overall time course of inactivation, making the channel II current appear to inactivate with a single exponential time course (*compare* Fig. 4 records to those in Figs. 1–3). As was the case with divalent inward currents (*see* Fig. 3*D*), inactivation time constants for the outward current in divalent-free solutions were well predicted from the time constants for the inward current inactivation at more negative potentials (*not shown*). It is possible that these effects are explained in part by a greater contribution of efflux through channel I to the net outward current in reduced external divalent levels.

Unitary Currents Corresponding to Channels I and II

We could not resolve single-channel currents corresponding to channels I and II in cell-attached patches using 50 mM Ca^{2+} or Ba^{2+} as the charge carrier. We therefore used divalent-free solutions (0 mM Ca, 0 mM Mg, 2 mM EGTA or BAPTA) in the patch pipette so that Na^+ would permeate through the channels and give larger single-channel currents. Patches exposed to low divalent solutions were stable for prolonged periods. All experiments were done with simultaneous whole-cell and attached-patch recording, so that absolute potentials

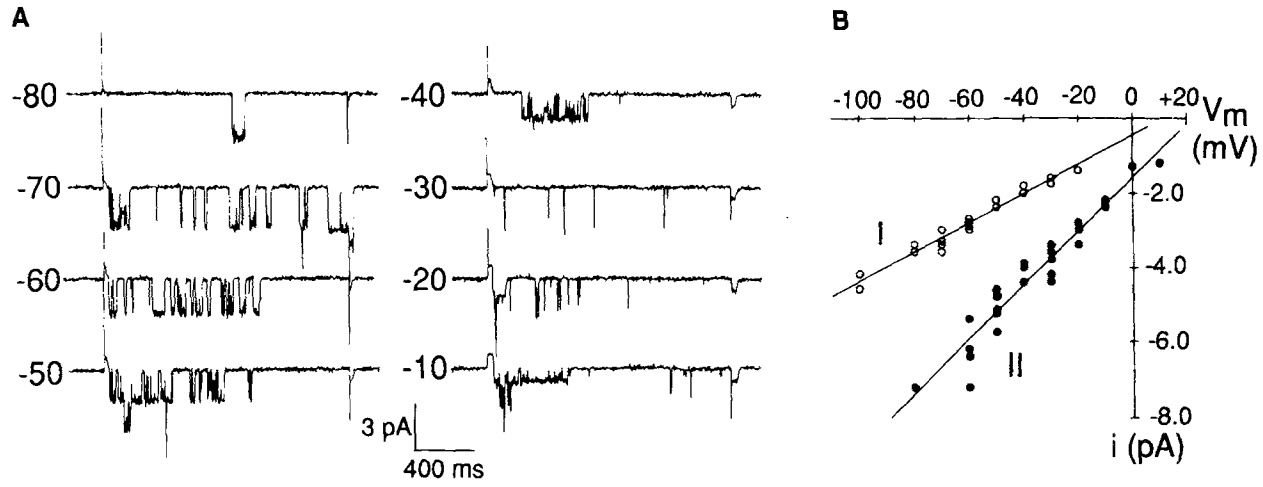

Fig. 5. Unitary currents corresponding to Na^+ influx through channels I and II. (*A*) Cell-attached patch recordings during pulses to the absolute potentials indicated. The pipette contained divalent-free ASW. The holding potential was −100 mV and pulses were applied to the whole-cell pipette. The records are not corrected for leakage or capacitative artifacts and are filtered at 2.9 kHz. Note the coexistence of channel I and II events in the traces taken at −50, −20 and −10 mV. (*B*) Current-voltage relations for the two types of unitary events. Each point represents the amplitude of one single-channel event

across the patch membrane were known. Pulses were applied to the whole-cell pipette, which minimized leakage currents across the patch pipette seal, and allowed us to monitor whole-cell currents at the same time as single-channel currents. The cell was bathed in 50 mM Ca external solution to increase whole-cell Ca^{2+} current amplitude.

In such experiments we consistently recorded two types of unitary inward currents which clearly corresponded to the channel I and II macroscopic currents. Figure 5*A* shows typical responses recorded in such an experiment. The cell was held at −100 mV, and 1.6-sec pulses were applied to the whole-cell pipette at 8-sec intervals. Beginning at voltages positive to −80 mV, long open-time single channels were seen which tended to open throughout the duration of the pulse at negative potentials and to cluster toward the pulse onset at more positive potentials. As the cell was depolarized to voltages more positive than −60 mV, a second inward unitary current type was seen, which was readily distinguishable from the low threshold channel by its larger amplitude and much shorter open time. At voltages positive to −60 mV, both channel types were often seen in single sweeps. It was unusual to find patches with only one of the two channel types present, although occasionally the channel I would disappear from a patch after prolonged recording.

Open channel *I-V* relations for the two types of single-channel currents are shown in Fig. 5*B*. These were obtained by measuring unitary current amplitudes at various potentials; since many of the high threshold channel openings were so brief as to be incompletely resolved, longer openings which were clearly recorded at full amplitude were selected. The slopes of these two plots correspond to conductances of 40 pS for the low threshold, long open-time channel, and 75 pS for the high threshold, short open-time channel. We could occasionally detect channel II unitary outward currents at positive potentials, but their fast kinetics made analysis very difficult.

Since only two inward currents are seen in whole-cell recordings, and only two types of single-channel currents are seen in patch recordings, we believe that the low threshold, long open-time channel corresponds to the channel I whole-cell current, and the high threshold, short open-time channel to the channel II macroscopic current.

Further evidence that the two types of unitary currents correspond to the channel I and II macroscopic currents comes from observations of the voltage dependence of steady-state inactivation in patches that contained both channel types. Figure 6 shows records taken from a patch during depolarizing pulses from holding potentials of −100 and −80 mV. Stepping from −100 mV, both channel types were seen, the smaller conductance, longer open-time channel at more negative potentials, and the larger, shorter open-time channel at more positive potentials. At −80 mV, however, channel I was selectively inactivated while the probability of opening of channel II at higher voltages was essentially unchanged. The patch holding potentials required to completely inactivate channel I are well predicted from the inactivation *vs.* voltage curve for channel I in 50 mM Ca external solution corrected for the surface potential shift observed in divalent-free external solutions.

Separation of channel I and II events can also be done on the basis of the correlation between long open time and low conductance. In many patches,

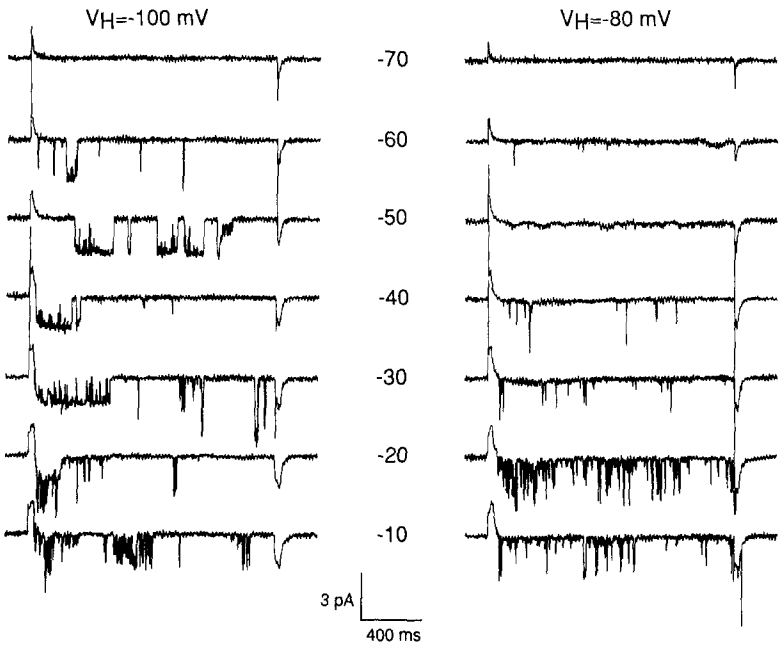

Fig. 6. Separation of channel I and II unitary currents by holding potential. Two sets of attached-patch recordings are shown, taken from a single patch during pulses to the potentials indicated from holding potentials of −100 mV (left) and −80 mV (right). The patch pipette contained divalent-free ASW. Holding potential was controlled and pulses delivered through the whole-cell pipette. Traces are not corrected for leakage or capacitative artifacts and are filtered at 2.9 kHz

at potentials between −60 and −30 mV, channel I and II events are detected in single sweeps. Figure 7*A* shows an amplitude histogram from a series of sweeps in one such patch at −40 mV. The channel I currents are apparent as a distinct peak centered at −1.9 pA. The channel II currents appear as a less distinct peak centered at approximately −3.2 pA; this peak is blurred by the truncation of many channel II events by the frequency response of the recording system. An open-time histogram of all events in this patch can be well described by the sum of two exponentials, with time constants of 0.75 and 6.14 msec (Fig. 7*B*). If these two exponentials represent the separate open-time characteristics of channels I and II, then large amplitude should be positively correlated with short open time. To test this, we determined the open-time histogram for all events in this patch with amplitudes greater than −2.6 pA, which excludes about 90% of the channel I events. This histogram is shown in Fig. 7*C*, and yields a single exponential with a time constant of 1 msec, close to the shorter time constant of the histogram for all events. As will be shown below, the open-time histogram for selected channel I events can be described with a time constant that corresponds to the longer (6 msec) time constant obtained from all events in Fig. 7*B*.

By averaging sweeps containing channels I and II at voltages throughout the activation range for both currents, we were able to reconstruct macroscopic currents that corresponded closely to those recorded from the same oocyte with the whole-cell pipette (Fig. 8). A patch was chosen which contained 5–10 channels of each type, a sufficiently small number so that individual events could be resolved at most potentials, but large enough so that macroscopic currents could be reconstructed from a relatively small number of sweeps. (The slow recovery from inactivation of channel I necessitated interpulse intervals of 8–10 sec.) Figure 8*A* shows averaged sweeps (10 sweeps/average) at voltages between −70 and +20 mV. The average currents reproduce the macroscopic channel I and II currents recorded in divalent-free external solutions reasonably well (*see* Fig. 4), given the small number of sweeps used for the averages. The *I-V* relation obtained from the peak average currents is shown in Fig. 8*B*, and is compared to the *I-V* relation obtained from whole-cell currents in this cell recorded at the same time. The average *I-V* relation from the patch matches the shape of the relation from the whole cell, and shows a negative surface potential shift similar to that previously estimated from sequential exposure of whole cells to 50 mM Ca and divalent-free external solutions.

Ca^{2+} and Mg^{2+} Block of Monovalent Permeation Through Channel I

Data presented above show that external Ca^{2+} and Mg^{2+} block monovalent permeation through both Ca^{2+} channels in the oocyte. The conductance of

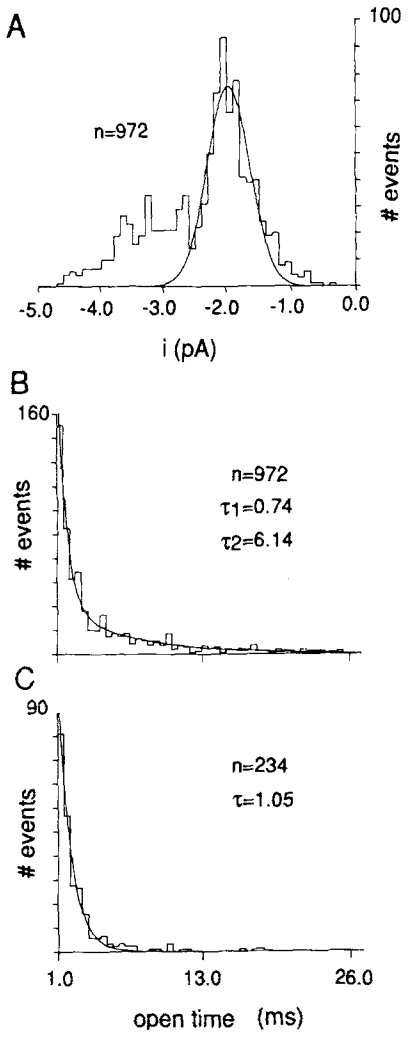

Fig. 7. Separation of channel I and II currents on the basis of the correlation between amplitude and open time. (*A*) Amplitude histogram of all events from a series of records taken during pulses to −40 mV in a patch which contained both types of unitary events (pipette solution: divalent-free ASW). The smooth curve is a best fit Gaussian distribution to all points of less than 2.6 pA in amplitude. (*B*) Open-time histogram for all events. The best fit curve has two exponentials with time constants of 0.74 and 6.14 msec. (*C*) Open-time histogram of events greater than 2.6 pA in amplitude, which excludes most channel I events. The best fit curve is a single exponential with a time constant of 1.05 msec

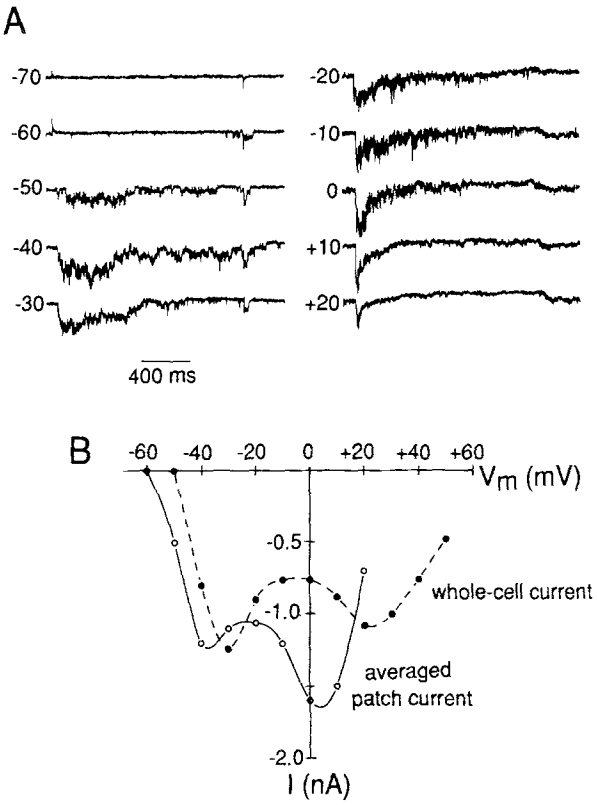

Fig. 8. Comparison of averaged single-channel records and whole-cell currents from the same cell. (*A*) Average of 10 sweeps at each potential indicated, in an attached-patch (pipette: divalent-free ASW) recording which had several active channels of each type. Pulses were delivered through the whole-cell pipette. Holding potential was −100 mV. (*B*) *I-V* relation of peak currents in *A* (○) and for whole-cell currents from the same cell taken at the same time (●; external solution: 50 Ca ASW). The shift between the two relations is similar to that estimated from sequential whole-cell recordings in 50 Ca and divalent-free ASW. The vertical scale for the averaged currents is arbitrary

channel I was large enough, and its open time sufficiently long in the absence of dihydropyridine agonists to allow us to quantify these effects at the single-channel level, and to determine individual rate constants for divalent binding to the channel.

Figure 9 shows single-channel I currents with 0, 50, and 200 μM Mg^{2+} in the patch pipette (0 mM Ca, 2 mM BAPTA) for all records. As the Mg^{2+} concentration was increased, the single-channel currents were interrupted more frequently by blocking events. Channel openings were not well resolved at Mg^{2+} concentrations greater than 500 μM. Histograms of open and closed times for 0 and 200 μM Mg^{2+} are shown in Fig. 10*A*. Both were well fitted with single exponentials at all levels of Mg^{2+}, consistent with there being a single open and single blocked state of the channel. (The longer closed intervals representing the times between bursts were ignored in calculating the fits.) Plots of blocking rate constants (reciprocal open times) and unblocking rate constants (reciprocal closed times within bursts) *vs.* [Mg^{2+}] are shown in Fig. 10*B*. As expected from a simple reaction scheme, the blocking rate is strongly concentration dependent, while the unblocking rate is essentially invariant with concentration. The slope of the blocking rate *vs.* [Mg^{2+}] relation is 6.4×10^6 M^{-1} sec^{-1}.

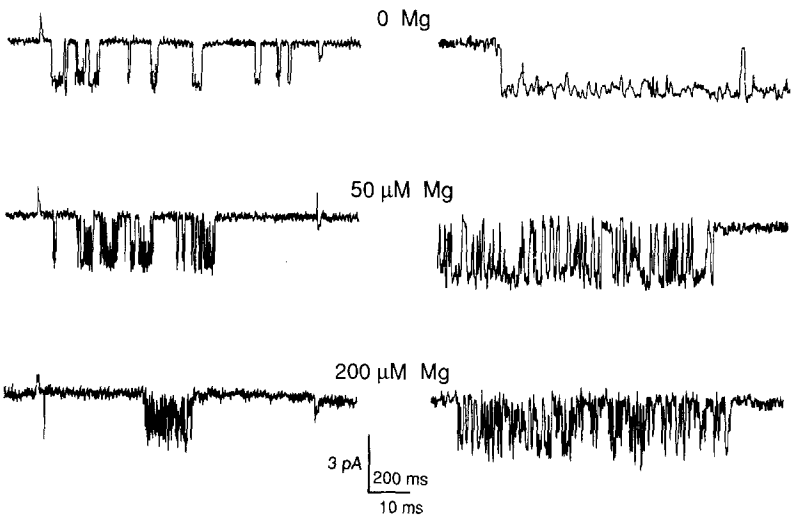

Fig. 9. Block by external Mg^{2+} of unitary events representing Na^+ influx through channel I. Records were taken during a voltage-clamp pulse to −60 mV (delivered through the whole-cell pipette) from a holding potential of −100 mV in three different patches at the patch pipette Mg^{2+} concentrations indicated. Traces are shown at two different time scales

A similar, though less complete analysis was carried out for the blocking effects of external Ca^{2+} ions. Three patches were analyzed, one at 0.5 μM Ca^{2+} and two at 1 μM. Open-time histograms for these patches were described by single exponentials with time constants of 3.8 msec (0.5 μM) and 1.7 and 1.5 msec (1 μM). A regression line including the rate constants derived from these values and three additional patches in 0 mM Ca (t_{open} = 6.3, 8.34 and 5.2 msec) had a slope of 4.5×10^8 M^{-1} sec^{-1}. This rate coefficient for Ca^{2+} entry agrees very closely with that derived for Ca^{2+} channels in ventricular muscle (Lansman et al., 1986).

Voltage Dependence of the Ca^{2+} and Mg^{2+} Block

We examined the voltage dependence of Ca^{2+} and Mg^{2+} block of Na^+ permeation through channel I in four patches. Figure 11 shows single-channel records taken in 0.5 μM Ca or 50 μM Mg at −40 and −60 mV. A clear difference between the Ca^{2+} and Mg^{2+} blocking actions is apparent in these records: whereas voltage has little effect on the Mg^{2+} block, the Ca^{2+} block appears to be substantially relieved at the more negative potential. This observation is consistent with the idea that negative voltages favor the exit of Ca^{2+} from its binding site within the channel toward the interior of the cell. Such an effect is not seen for Mg^{2+}, which is relatively impermeant in the channel and therefore cannot readily exit into the cell interior (*see* Fukushima & Hagiwara, 1985).

Discussion

We have described two voltage-dependent calcium currents in unfertilized oocytes of the ascidian *Ciona intestinalis*, at both the macroscopic and single-channel levels. The two currents are distinguishable by their voltage dependencies of activation and inactivation, their rates of inactivation, and their permeability sequences for divalent cations. Both calcium channels permit permeation of monovalent cations when divalent levels are reduced. Using divalent-free solutions to increase the amplitude of single-channel currents, we could record unitary events corresponding to the two currents, which were distinguishable by their different conductances and open times. Interruptions of single channel I currents corresponding to the Ca^{2+} and Mg^{2+} block of Na permeation were recorded and rate constants characteristic of the block determined.

The Ca^{2+} channels in *Ciona* bear a superficial similarity to low- and high-threshold Ca^{2+} channels in vertebrate cells, though they do not fall readily into this classification scheme. The *Ciona* channel I resembles the low voltage-activated, or T-type, channel of vertebrate sensory neurons (Carbone & Lux, 1987; Fox et al., 1987) in that it is activated at potentials only slightly positive to the resting potential of the cell and can be separated from the high voltage-activated current by its inactivation at relatively negative holding potentials. The unitary conductances in Na^+ for the *Ciona* channels are similar to those in vertebrate cells (*Ciona* channel I, 40 pS; chick DRG 1.v.a. channel, 24 pS: Lux, Carbone & Zucker, 1989; *Ciona* channel II, 75 pS; cardiac L

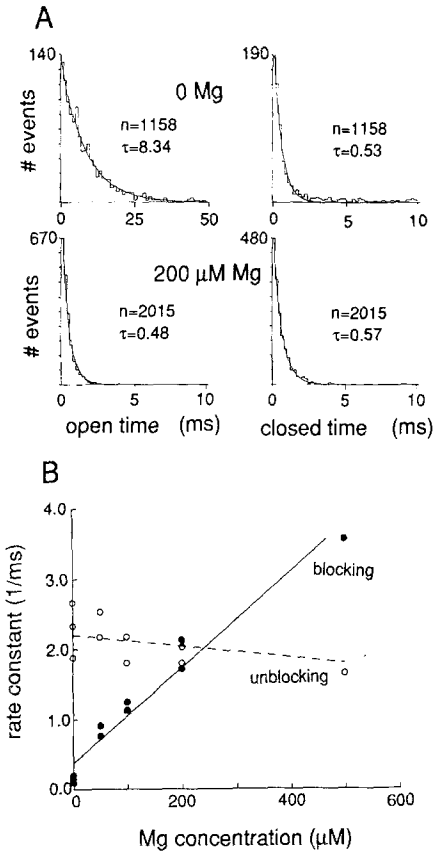

Fig. 10. Kinetics of the Mg^{2+} block of channel I monovalent influx. (*A*) Open-time (left) and closed-time (right) histograms from two patches with pipette Mg^{2+} concentrations of 0 and 200 μM, taken at a potential of −60 mV. Note that the horizontal scale of the open-time histogram in 0 Mg^{2+} is different from the others. The fits to the closed-time histograms exclude the small contribution from longer closed intervals that represent gaps between bursts. (*B*) Plots of blocking rate (●; reciprocal open time) and unblocking rate (○; reciprocal closed time) *vs.* [Mg^{2+}]

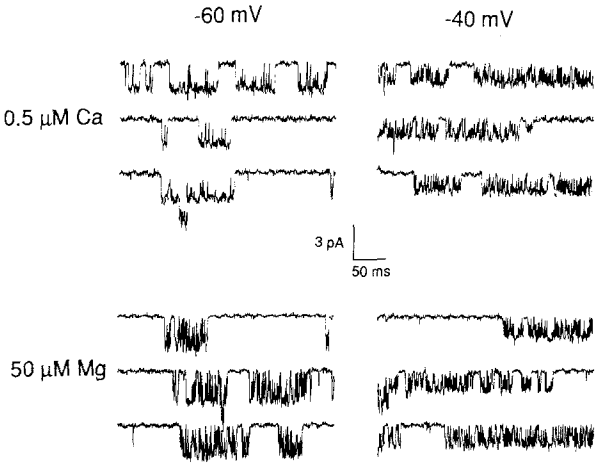

Fig. 11. Voltage dependence of Ca^{2+} and Mg^{2+} block of channel I Na^+ permeation. (*A*) Single-channel records from two patches with 0.5 μM Ca^{2+} or 50 μM Mg^{2+} in the patch pipette taken at −60 and −40 mV. Note the relief of the block at −60 mV for Ca^{2+}, but not for Mg^{2+}

channel, 85 pS: Hess et al., 1986). The mean open times for *Ciona* channel I, however, are considerably longer than those measured at similar potentials for low threshold vertebrate channels (Lux et al., 1989). In contrast to the T-type channel, which shows approximately equal macroscopic conductances in Ca^{2+} and Ba^{2+} (Fox et al., 1987), the *Ciona* channel I conductance is much larger in Ba^{2+} than in Ca^{2+}. The *Ciona* channel II shows about equal conductance in Ba^{2+} and Ca^{2+}, while the N- and L-type channels are more conductive in Ba^{2+}.

Despite these differences, the *Ciona* Ca^{2+} channels share many of the basic permeation mechanisms with vertebrate Ca^{2+} channels. As is the case for the cardiac L-type (Lansman et al., 1986), and hybridoma channels (Fukushima & Hagiwara, 1985), which are the most extensively characterized, occupancy of a divalent cation binding site with an affinity for Ca^{2+} in the micromolar range and Mg^{2+} in the millimolar range, prevents monovalent flux through the channel. Removal of divalents from the external solution in *Ciona* thus results in Na^+ influx through both Ca^{2+} channels. Removal of divalents from the site in normal external solutions at positive voltages results in K^+ efflux through at least one of the two channels. In agreement with results in ventricular muscle (Hess & Tsien, 1984), hybridoma cells (Fukushima & Hagiwara, 1985), GH_3 cells (Suarez-Kurtz, Katz & Reuben, 1987), skeletal muscle (Almers et al., 1984) and snail neurons (Kostyuk & Krishtal, 1977), Na^+ currents through both *Ciona* Ca^{2+} channels are very large compared to Ca^{2+} currents. This indicates that, in agreement with several models of the Ca^{2+} channel, permeation occurs *via* ion binding. Thus ions with low relative permeability, such as Na^+, have relatively high mobility in the channel because of their weak binding at the site with high affinity for divalent ions. In addition, when comparing two permeant divalents, such as Ca^{2+} and Ba^{2+}, there is a correlation between large outward monovalent flux through the Ca^{2+} channel and more negative reversal potentials between inward and outward currents. This can be explained if the efflux of monovalents occurs because of the voltage-dependent unbinding of the divalent from a high affinity site in the channel; ions such as Ba^{2+}, that carry larger currents due to their high mobility in the channel unbind at more negative voltages. In further agree-

ment with work on several of the above cell types (Kostyuk et al., 1983; Almers et al., 1984; Hess & Tsien, 1984), we find a difference of at least three orders of magnitude in the apparent binding affinities for Ca^{2+} of the site that prevents monovalent permeation and the site that determines Ca^{2+} permeation itself. The first value is determined from single-channel data taken in the presence of micromolar levels of external Ca^{2+}, and the latter from the lack of saturation of either inward current at 10 mM external Ca^{2+}, since both channel I and II macroscopic currents were increased when external Ca^{2+} was raised from 10 to 50 mM. This discrepancy in affinities indicates that there are two binding sites for Ca^{2+} within the channel. The apparent difference in binding constants for Ca^{2+} could be attributed either to true differences between the two sites (Kostyuk & Krishtal, 1977), or to electrostatic repulsion between Ca^{2+} ions bound to two similar sites within the channel (Lansman et al., 1986).

Single-channel studies of the Ca^{2+} or Mg^{2+} block of monovalent permeation are generally difficult because of the short open times of most Ca^{2+} channels. In some channels, dihydropyridine agonists can be used to promote long openings and facilitate measurement of the blocking and unblocking events (Hess, Lansman & Tsien, 1984). We were able to study Ca^{2+} and Mg^{2+} binding to channel I at the single-channel level in the absence of dihydropyridine agonists, because of the relatively long mean open time of the unmodified channel. Our results are in close agreement with those for the Bay K-modified cardiac L-type channel (Lansman et al., 1986) in showing that micromolar concentrations of Ca^{2+} reduce the open time of the channel. For the *Ciona* channel I and the cardiac L channel, plots of blocking rate constant for the Ca^{2+} block *vs.* $[Ca^{2+}]$ had identical slopes, yielding primary rate constants of 4.5×10^8 M^{-1} sec^{-1}. In the absence of Ca^{2+} and Mg^{2+}, the average mean open times were similar for the L channel (in the presence of Bay K; 5.9 msec; Lansman et al., 1986) and the *Ciona* channel I (6.6 msec). Our results differ from those of Lux et al. (1989) on the chick l.v.a. channel, who observed that the main effect of Ca^{2+} at low concentrations (0.1–10 μM) was to increase the duration of channel closures, and only at high concentrations (50 μM) was a reduction in open time due to blocking effects observed. In the *Ciona* channel I, binding of Mg^{2+} was approximately 70-fold less strong than Ca^{2+}.

In our results, the Ca^{2+} block was relieved at negative potentials, as was the case for the cardiac L channel and the hybridoma channel (Fukushima & Hagiwara, 1985). This was attributed to the fact that Ca^{2+}, being permeant in the channel, could come off the binding site toward the cell interior at negative potentials. In agreement with data from the hybridoma channel, we have confirmed that in the *Ciona* channel I, there was no relief of the block by Mg^{2+}, an impermeant ion, at negative potentials. In the cardiac L channel, the Mg^{2+} block of unitary Ba^{2+} currents was accentuated at negative voltages, due to an increased on-rate, as expected for a binding site which senses the electrical field across the membrane (Lansman et al., 1986). This was studied over a range of voltages positive to those in our experiments, so we cannot make a direct comparison with our results.

Although Ca^{2+} currents have been studied extensively in oocytes at the macroscopic level, very few single-channel studies have been reported (Bountra & Martin, 1987). In mouse oocytes, monovalent permeation through Ca^{2+} channels in low divalent external solutions has been demonstrated under both current-clamp (Yoshida, 1983) and voltage-clamp conditions (Peres, 1987). The transient outward current recorded at positive potentials in mouse oocytes has also been attributed to K^+ efflux through Ca^{2+} channels (Peres, 1987).

Our results clearly show that despite many differences between oocyte Ca^{2+} channels and those in mature cells, some of the most basic permeation characteristics are the same. We know from previous studies that Ca^{2+} currents in ascidian embryos can undergo complex changes during development (Hirano & Takahashi, 1984), including changes that are specific to certain embryonic cell lineages (Simoncini et al., 1988). It will be interesting to determine at the single-channel level the basis for these changes.

We dedicate this paper to the late Professor Susumu Hagiwara. We thank the members of the Department of Physiology, University of Bristol, for their hospitality during our visit. We are particularly grateful to R.C. Thomas and R.W. Meech for arranging and financing the visit, and to R.W. Meech for providing laboratory facilities for the experiments. J.F. Ashmore loaned essential supplies, sometimes knowingly. B.M.H. Bush provided animal holding facilities. Q. Bone at the Marine Laboratory, Plymouth, kindly helped us obtain *Ciona*. M.M.B. was supported by a grant from the MRC to R.W. Meech. W.J.M. was supported by a travel fellowship from the Royal Society, by NIH grant HD 17486, and by a Research Career Development Award from the NIH.

References

Almers, W., McCleskey, E.W. 1984. Non-selective conductance in calcium channels in frog muscle: Calcium selectivity in a single-file pore. *J. Physiol. (London)* **353**:585–608

Almers, W., McCleskey, E.W., Palade, P.T. 1984. A non-selec-

tive conductance in frog muscle membrane blocked by micromolar external calcium ions. *J. Physiol. (London)* **353:**565–583

Block, M.L., Moody, W.J. 1987. Changes in sodium, calcium and potassium currents during early embryonic development of the ascidian, *Boltenia villosa*. *J. Physiol. (London)* **393:**619–634

Bountra, C., Martin, R.J. 1987. Single-channel currents from zona-free mouse eggs. *Q. J. Exp. Physiol.* **72:**483–492

Carbone, E., Lux, H.D. 1987. Kinetics and selectivity of a low-voltage-activated calcium current in chick and rat sensory neurones. *J. Physiol. (London)* **386:**547–570

Deitmer, J.W. 1984. Evidence for two voltage-dependent calcium currents in the membrane of the ciliate *Stylonychia*. *J. Physiol. (London)* **355:**137–159

Fedulova, S.A., Kostyuk, P.G., Veselovsky, N.S. 1985. Two types of calcium channels in the somatic membrane of newborn rat dorsal root ganglion neurones. *J. Physiol. (London)* **359:**431–446

Fox, A.P., Nowycky, M.C., Tsien, R.W. 1987. Kinetic and pharmacological properties distinguishing three types of calcium currents in chick sensory neurones. *J. Physiol. (London)* **394:**149–172

Fukushima, Y., Hagiwara, S. 1985. Currents carried by monovalent cations through calcium channels in mouse neoplastic B lymphocytes. *J. Physiol. (London)* **358:**255–284

Hagiwara, S., Ozawa, S., Sand, O. 1975. Voltage-clamp analysis of two inward current mechanisms in the egg cell membrane of a starfish. *J. Gen. Physiol.* **65:**617–644

Hagiwara, S., Yoshii, M. 1979. Effects of internal potassium and sodium on the anomalous rectification of the starfish egg as examined by internal perfusion. *J. Physiol. (London)* **292:**251–265

Hamill, O.P., Marty, A., Neher, E., Sakmann, B., Sigworth, F.J. 1981. Improved patch clamp techniques for high-resolution current recording from cells and cell-free membrane patches. *Pfluegers Arch.* **391:**85–100

Hess, P., Lansman, J.B., Tsien, R.W. 1984. Different modes of Ca^{2+} channel gating behavior favoured by dihydropyridine agonists and antagonists. *Nature (London)* **311:**538–544

Hess, P., Lansman, J.B., Tsien, R.W. 1986. Calcium channel selectivity for divalent and monovalent cations. Voltage and concentration dependence of single channel current in ventricular heart cells. *J. Gen. Physiol.* **88:**293–319

Hess, P., Tsien, R.W. 1984. Mechanism of ion permeation through calcium channels. *Nature (London)* **309:**453–456

Hice, R.E. 1988. Electrophysiology of Ascidian Oocytes. Ph.D. Thesis. University of Washington, Seattle

Hirano, T., Hagiwara, S. 1989. Kinetics and distribution of voltage-gated Ca, Na and K channels on the somata of rat cerebellar Purkinje cells. *Pfluegers Arch.* **413:**463–469

Hirano, T., Takahashi, K. 1984. Comparison of properties of calcium channels between the differentiated 1-cell embryo and the egg cell of ascidians. *J. Physiol. (London)* **347:**301–325

Kostyuk, P.G., Krishtal, O.A. 1977. Effects of calcium and calcium-chelating agents on the inward and outward current in the membrane of mollusc neurones. *J. Physiol. (London)* **270:**569–580

Kostyuk, P.G., Mironov, S.L., Shuba, Ya. M. 1983. Two ion-selecting filters in the calcium channel of the somatic membrane of mollusc neurons. *J. Membrane Biol.* **76:**83–93

Lansman, J.B., Hess, P., Tsien, R.W. 1986. Blockade of current through single calcium channels by Cd^{2+}, Mg^{2+}, and Ca^{2+}. Voltage and concentration dependence of calcium entry into the pore. *J. Gen. Physiol.* **88:**321–347

Lee, K.S., Tsien, R.W. 1982. Reversal of current through calcium channels in dialysed single heart cells. *Nature (London)* **297:**498–501

Lux, H.D., Brown, A.M. 1984. Patch and whole cell calcium currents recorded simultaneously in snail neurons. *J. Gen. Physiol.* **83:**727–770

Lux, H.D., Carbone, E., Zucker, H. 1989. Block of Na^+ ion permeation and selectivity of Ca channels. *Ann. NY Acad. Sci.* **560:**94–102

Matteson, D.R., Armstrong, C.M. 1986. Properties of two types of calcium channels in clonal pituitary cells. *J. Gen. Physiol.* **87:**161–182

Narahashi, T., Tsunoo, A., Yoshii, M. 1987. Characterization of two types of calcium channels in mouse neuroblastoma cells. *J. Physiol. (London)* **383:**231–249

Peres, A. 1987. The calcium current of mouse egg measured in physiological calcium and temperature conditions. *J. Physiol. (London)* **391:**573–588

Simoncini, L., Block, M.L., Moody, W.J. 1988. Lineage-specific development of calcium currents during embryogensis. *Science* **242:**1572–1575

Suarez-Kurtz, G., Katz, G.M., Reuben, J.P. 1987. Currents carried by sodium ions through transient calcium channels in clonal GH3 pituitary cells. *Pfluegers Arch.* **410:**345–347

Tsien, R.Y. 1980. New calcium indicators and buffers with high selectivity against magnesium and protons: Design, synthesis and properties of prototype structures. *Biochemistry* **19:**2396–2412

Tsien, R.W., Hess, P., McCleskey, E.W., Rosenberg, R.L. 1987. Calcium channels: Mechanisms of selectivity, permeation, and block. *Annu. Rev. Biophys. Biophys. Chem.* **16:**265–290

Tsien, R.W., Lipscombe, D., Madison, D.V., Bley, K.R., Fox, A.P. 1988. Multiple types of neuronal calcium channels and their selective modulation. *Trends Neurosci.* **11:**431–438

Yoshida, S. 1983. Permeation of divalent and monovalent cations through the ovarian oocyte membrane of the mouse. *J. Physiol. (London)* **339:**631–642

Received 19 July 1989; revised 17 October 1989